Journal of Materials Chemistry A

Accepted Manuscript

ROYAL SOCIETY OF CHEMISTRY

www.rsc.org/materialsA

Triptycene based 1,2,3-Triazole linked Network Polymers (TNPs) : Small Gas Storage and Selective CO_2 Capture

Snehasish Mondal and Neeladri Das*

Department of Chemistry, Indian Institute of Technology Patna, Patna 800 013, Bihar, India

E-mail: neeladri@iitp.ac.in, neeladri2002@yahoo.co.in; Tel.: +91 9631624708

Abstract

Herein, facile synthesis and characterization of four Triazole linked Network Polymers (**TNP**s) in high yields is described. These nitrogen rich polymers are derived using "Click" reaction between 2,6,14-triazido triptycene and various di or triethynyl comonomers. The **TNP**s are microporous and exhibit high surface area (SA_{BET} up to 1348 m^2g^{-1}). Due to incorporation of 1,2,3-triazole motif (a CO_2-philic moiety), the **TNP**s record moderate to high CO_2 uptake (upto 4.45 mmol/g at 273K and 1 bar). The **TNP**s also show very good CO_2/N_2 (upto 48) and CO_2/CH_4 (8 - 9) selectivity. While highest storage capacity has been registered by **TNP4** (CO_2 4.45 mmol/g at 273K and 1 bar, CH_4 23.8 mg/g, H_2 1.8 wt%), the highest CO_2/N_2 and CO_2/CH_4 selectivity was shown by **TNP3** which contains additional nitrogen rich building blocks in the form of heteroaromatic pyrazine rings. These results suggest that **TNP**s are porous materials with potential practical application in gas storage and separation.

Introduction:

Design and syntheses of porous materials have attracted considerable research attention over the past decade.[1-4] In recent years, research output in this direction has witnessed considerable growth.[5-13] Depending on the pore size, porous materials may be classified as ultra-microporous[14-16] microporous,[12,13] mesoporous[17-19] or macroporous.[20,21] Among these, microporous materials have emerged as potential candidates for applications that include but are not limited to gas storage and separation. Microporous materials, such as zeolites[22,23] and metal-organic frameworks (MOFs),[1-5] contain metal atoms. Alternatively, microporous materials can also be designed in the form of metal-free organic polymers that are highly crosslinked. Acronyms such as COFs, CMPs, CTFs, EOFs, HCPs, MOPs, OCFs, PAFs, PIMs, POFs, POPs, PPFs, PPNs, etc have been coined to describe metal-free porous organic polymers.[6-13] In general, MOFs have limited industrial applications as porous materials because presence of relatively labile coordination bonds that lower their thermal stability.[24] On the other hand, in microporous organic polymers (MOPs), light weight elements (such as H, C, N, and O) are interlinked via relatively stronger covalent bonds. Therefore these metal-free materials have lesser mass densities and higher stabilities (chemical and thermal). In addition, MOPs can be easily tailored with respect to properties such as guest selectivity and pore properties, due to availability of a plethora of multifunctional organic molecules that can serve as monomers towards the syntheses of MOPs.

In contemporary research dealing with development of microporous materials, design of MOPs for selective CO_2 capture and sequestration has received special attention.[24-46] This has stemmed from environmental and energy concerns related to CO_2, which is a major greenhouse gas. It is well known that thermal power plants emitting flue gas (containing approximately 15 % CO_2) are a major contributor to anthropogenic CO_2. Therefore, in order to contain global climate warming arising out of anthropogenic CO_2 emissions, there is a pressing demand to develop novel materials that can efficiently and selectively adsorb large quantities of CO_2 emitted from fossil-fuel fired power plants (classified as fixed-point CO_2 emission sources). Also it is desirable to separate CO_2 (present as an impurity) from natural gas that

contains 80-95 % methane.[47,48] This explains the growing research interest to design MOPs having practical applications such as selective capture and sequestration of CO_2.

As far as the design of polymers for better CO_2 adsorption and gas selectivity is concerned, it has been reported that incorporation of polar groups in the framework of porous organic polymers not only enhances carbondioxide uptake but also improves its selectivity over methane and nitrogen. This enhancement in CO_2 uptake is attributed to van der Waals interactions (quadrupole-dipole interactions and/or hydrogen bonding) between CO_2 and the polar functional groups that are present in the backbone of MOPs. Additionally, polymeric networks synthesized from electron rich monomers may also exhibit higher CO_2 uptake. This property is attributed to favorable Lewis acid-base interactions between the electron deficient carbon atom in CO_2 and the relatively electron rich polymer.[49,50]

1,2,3-triazole is a nitrogen rich motif and it can be easily incorporated in the polymer framework by reacting monomers with multiple azide and ethynyl functional groups. Nguyen and co-workers have described synthesis of porous networks by covalently linking tetrahedral monomers using Click Chemistry.[33] Triazole molecules (1,2,3- and 1,2,4-triazole) may be considered CO_2–philic, considering the magnitude of their CO_2 binding energies.[51] It is therefore anticipated that polymers having these nitrogen rich moieties in their backbone may be potential candidates for efficient CO_2 sorption and separation. Triptycene on the other hand, is a robust and structurally rigid motif that has three dimensional orientation of three arene rings fused to a [2.2.2]bicyclooctatriene moiety. Triptycene based porous polymers have often exhibited good gas storage and separation properties.[52-58] This is often attributed to the "internal molecular free volume (IFV)" that arises from the inefficient packing of rigid three dimensional units of triptycene present in the polymer backbone.[52,55,57,58]

With these premises in mind, we were interested in designing network polymers that would contain both 1,2,3-triazole motif (as polar groups) and triptycene motif (as a bulky rigid group). It is anticipated that such polymeric networks would be porous and simultaneously exhibit reasonably high uptake of CO_2, primarily because of CO_2–philic nature of polar 1,2,3-triazole moiety and the porosity arising from the inefficient packing of the triptycene units in the polymers.

Herein, we report synthesis of a series of new triptycene based and 1,2,3-triazole linked network polymers (**TNP**s) using 2,6,14-triazidotriptycene and various di- and tri ethynyl substituted comonomer via Cu(I)OAc catalyzed "Click" reaction. Complete structural characterization of these polymers and their performance as materials for gas storage as well as selective gas uptake has been described elaborately. **TNP**s constructed from monomers with three ethynyl functional groups, have a relatively higher surface area in comparison to **TNP**s derived from diethynyl comonomers. However, all **TNP**s exhibit microporosity (pore diameter < 2 nm). Additionally, these microporous **TNP**s also demonstrated similar or even better carbondioxide storage ability and selectivity than a wide range of the previously reported MOPs.

Experimental section

Materials and methods: Triptycene, aromatic bromides and Cu(I)OAc were obtained from Sigma Aldrich and were utilized without further purification. 2,6,14-triazodotriptycene was prepared from triptycene using literature reported protocol.[59] All the aromatic ethynyl compounds were synthesized from corresponding aromatic bromide using Sonogashira cross-coupling reaction.[60] Chromatographic purifications were performed using silica gel (100-200 mesh). Solid-state ^{13}C cross-polarization magic angle spinning (CP-MAS) NMR spectra were obtained using BRUKER 300 MHz (H-1 frequency) NMR spectrometer at a mass rate 8 kHz and CP contact time 2 ms with delay time 3 Sec. FTIR analyses were performed using Shimadzu IR Affinity-1 spectrometer. Elemental analyses were performed using vario MICRO cube analyser. P-XRD data were recorded using a Rigaku TTRAX III X-ray diffractometer.

Porosity analyses were performed using Quantachrome autosorb iQ_2 analyzer using UHP grade adsorbates. In a typical experiment, **TNP** (60 ~ 90 mg) was taken in a 9 mm large cell and attached to the degasser unit and degassed at 120 ºC for 12-24 hr. The samples were refilled with helium and weighed carefully and then the cells were attached to the analyzer unit. The temperature was maintained using KGW isotherm bath (provided by Quantachrome) filled with liquid N_2 (77K), or temperature controlled bath (298K and 273K).

Synthesis of TNP1: A typical experiment for the syntheses of **TNP**s, is described using **TNP1** as a representative example. 2,6,14-triazidotriptycene (189 mg, 0.5 mmol), 2,6,14-triethynyltriptycene (163 mg, 0.50 mmol) and Cu(I)OAc (4 mg, 0.03 mmol) were taken in a Schlenk flask under inert atmosphere. Degassed DMF (30 mL) was added to the flask with continuous stirring to dissolve the reactants. The flask (containing reactant) was subsequently heated at 120 ºC with vigorous stirring. After a few minutes of stirring, the reaction mixture assumed the form of a light yellow gelatinous precipitate. The reaction mixture was allowed to stir for additional 24 hours with the resultant formation of a large amount of gelatinous precipitate. The reaction mixture was cooled to room temperature and filtered through glass frit followed by washing with DMF, DMSO, acetone, THF and dichloromethane. The product thus obtained was dried under reduced pressure at 100 °C and crushed with a mortar and pestle to yield a brownish yellow powder.
Yield: 338 mg, 96%; FT-IR (KBr): 3404, 1660, 1464, 1221, 1035 cm^{-1}. Elemental Analysis: Calculated for $C_{46}H_{25}N_9$: C 78.51, H 3.58, N 17.91. Found: C 72.57, H 3.67, N 15.13.

Synthesis of TNP2: TNP2 has been prepared following the similar procedure as described for **TNP1** using 2,6,14-triazidotriptycene (189 mg, 0.5 mmol), 4,4'-diethynyl-biphenyl (152 mg, 0.75 mmol) and Cu(I)OAc (4 mg, 0.03 mmol). Unlike **TNP1**, large amount of yellow precipitate was observed after 24 hours stirring at 120 °C. After drying at reduced pressure at 120 °C, the final product was obtained as a light yellow powder.
Yield: 300 mg, 88%; FT-IR (KBr): 3400, 1606, 1477, 1226, 1038 cm^{-1}. Elemental Analysis: Calculated for $C_{44}H_{26}N_9$: C 77.63, H 3.85, N 18.52. Found: C 71.97, H 4.36, N 15.93.

Synthesis of TNP3: This polymer was synthesized using 2,6,14-triazidotriptycene (189 mg, 0.5 mmol), 2,6-diethynylpyrazine (96 mg, 0.75 mmol) and Cu(I)OAc (4 mg, 0.03 mmol). Unlike other **TNP**s, formation of light brown fluffy precipitate was observed within a few minutes of stirring at 120 ºC. After 24 hours of stirring, formation of considerable amount of fluffy precipitate was observed. After drying at reduced pressure at 120 °C, the final product was obtained as light brown fluffy powder.
Yield: 242 mg, 85%; FT-IR (KBr): 1569, 1489, 1238, 1033 cm^{-1}. Elemental Analysis: Calculated for $C_{32}H_{17}N_{12}$: C 67.48, H 3.01, N 29.51. Found: C 62.36, H 3.61, N 25.93.

Synthesis of TNP4: This polymer was synthesized using 2,6,14-triazidotriptycene (189 mg, 0.5 mmol), 1,3,5-triethynylbenzene (75 mg, 0.50 mmol) and Cu(I)OAc (4 mg, 0.03 mmol). In this case, large amount of dark yellow gelatinous precipitation was observed after stirring for 24 hours. After drying at reduced pressure at 120 °C, the final product obtained as a dark brown solid. The solid product was then crushed in a mortar to yield the final product as a brownish yellow powder.
Yield: 259 mg, 98%; FT-IR (KBr): 3391, 1614, 1486, 1226, 1046 cm^{-1}. Elemental Analysis: Calculated for $C_{32}H_{17}N_9$: C 72.86, H 3.25, N 23.90. Found: C 65.74, H 4.09, N 20.82.

Result and discussion

Synthesis and characterization of TNPs.

The **TNP**s were synthesized utilizing the well known Cu(I) catalyzed Click reaction that is known to regioselectively yield the 1,4-disubstituted 1,2,3-triazole derivative. It is well documented in literature

that "standard" azide-alkyne click reactions, carried out in water or water/DMF mixture, utilize Cu(I) species generated in situ via reduction of $CuSO_4$ with sodium ascorbate. However, in recent years, copper (I) acetate is being used as the source of Cu(I) instead of $CuSO_4$/sodium ascorbate mixture, since the later catalytic system either yields insoluble products or reactions are sluggish in nature.[61] Chen and Guan reported Click polymerization using CuOAc (source of Cu^I) in DMF (as a solvent).[62] Based on this literature report, we have synthesized a series of 1,4-disubstituted 1,2,3-triazole bridged network polymers (**TNP**s) using 2,6,14-triazidotriptycene and various monomers containing multiple ethynyl functional groups as outlined in Scheme 1.

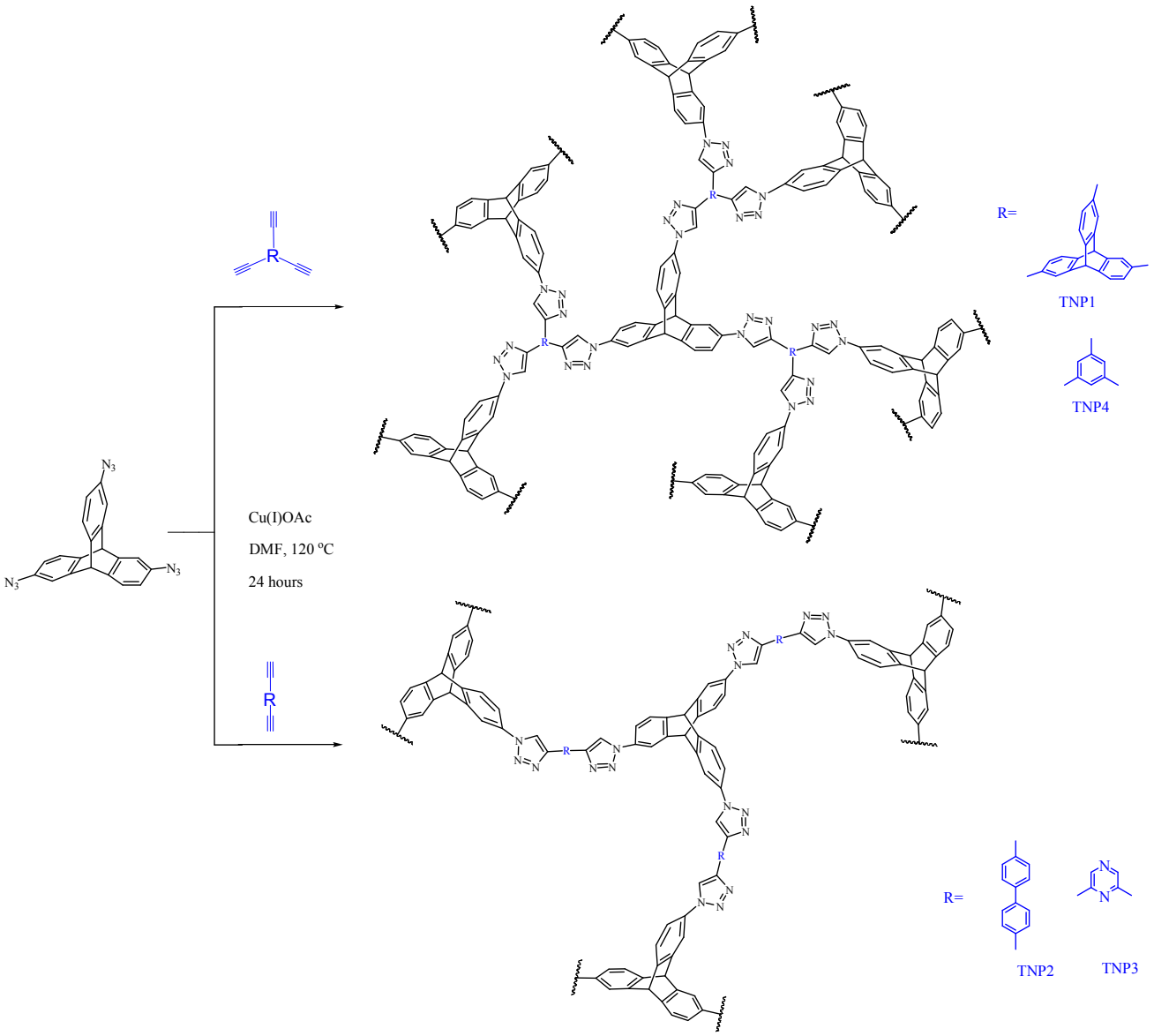

Scheme 1. Synthesis of **TNP1-TNP4**

In a typical reaction for the synthesis of **TNP**s, 2,6,14-triazidotriptycene,[59] the corresponding ethynyl monomer (di or triethynyl) and 6 mole % (with respect to 2,6,14-triazidotriptycene) Cu(I)OAc were dissolved in 30 ml of DMF and refluxed for 24 hours under N_2 atmosphere. In case of **TNP1** and **TNP4** that utilized triethynyl monomers, gelatinous precipitation was observed after completion of the reaction.

In this case, upon drying the precipitate under vacuum, the final product was obtained as brownish yellow solid. FESEM images of the product obtained for **TNP1** and **TNP4** revealed aggregated sheet like structure. On the other hand, in case of reactions leading to the formation of **TNP2** and **TNP3** (using diethynyl monomers in conjugation with 2,6,14-triazidotriptycene), the corresponding products precipitated as fluffy solid which were distinctly different from the gelatinous precipitates observed in case of **TNP1** and **TNP4**. As a consequence, for **TNP2** and **TNP3**, the FESEM images revealed presence of aggregated particles in their morphologies which was distinctly different from that observed in case of **TNP1** and **TNP4** (Figure 1). Wide-angle X-ray diffraction (WAXD) analyses of **TNP**s suggested that these polymeric materials are amorphous in nature due to the featureless broad nature of the diffraction pattern in each case (Figure 1). This amorphous nature of the TNPs is due to the rapid and irreversible formation of triazole linkage during polymerization.[12b]

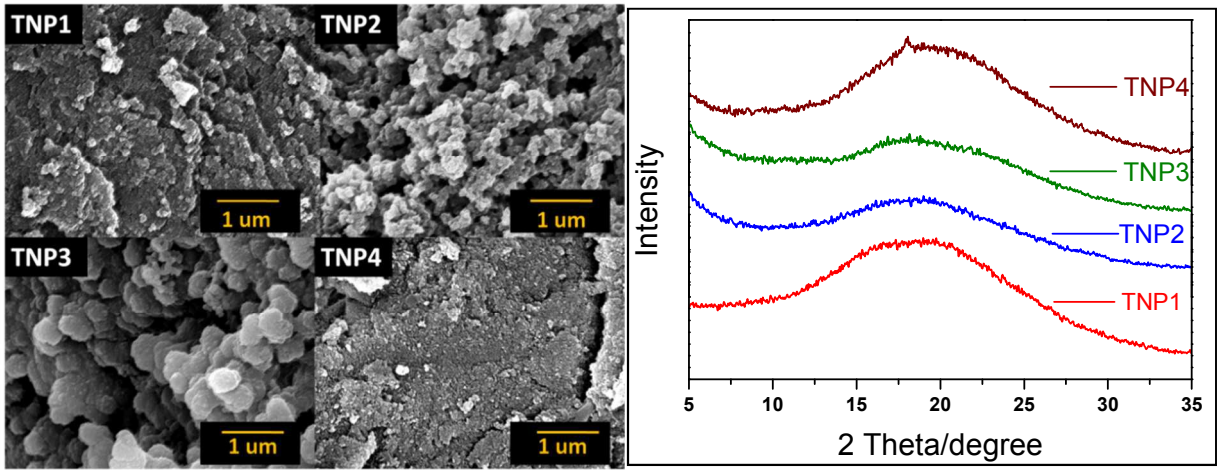

Figure 1. FESEM micrograph of **TNP1-TNP4** (Left); WAXD pattern of the **TNP1-TNP4** recorded at ambient temperature at a scan rate 3°/min (right)

The TNPs thus obtained were structurally characterized using solid state ^{13}C (CP-MAS) NMR, and Fourier transform infrared (FTIR) spectroscopy. The ^{13}C CP-MAS spectrum of **TNP4** has been shown as a representative example (Figure 2). The peak centered at 53 ppm corresponds to the bridgehead carbon of triptycene. The appearance of this peak is consistent with that of literature reported triptycene based monomer or polymers[54-57,59] thereby confirming the successful incorporation of triptycene motif in the polymer backbone. The peaks due to the phenyl ring carbons of the triptycene appear in the range 120-150 ppm. The resonance signal centered at 168 ppm is assigned to a carbon present in the 1,2,3-triazole motif, thereby confirming the formation of 1,2,3-triazole linkages via Click reaction. The ^{13}C CP-MAS spectra (Figure S1) of the other **TNP**s match well with that of **TNP4**, thereby supporting the formation of the desired polymers as shown in Scheme 1.

Polymerization has also been confirmed by FTIR spectroscopic data analysis (Figure S2). FTIR spectrum of **TNP2** is shown as a representative example in Figure 3. The characteristic band of azide functional group present in the triptycene monomer (2096 cm^{-1}) is absent in **TNP2**. Simultaneously, a band due to C−H stretching vibration of terminal alkynes (3280 cm^{-1}), observed in the corresponding diethynyl comonomer is missing in the FTIR spectrum of **TNP2**. This strongly suggests Click polymerization reaction between monomers containing terminal azide and terminal alkyne groups.

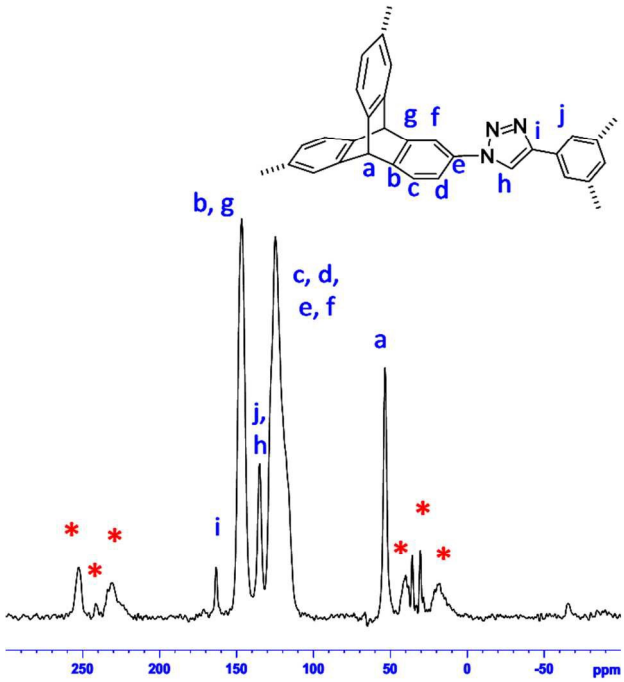

Figure 2. ^{13}C CP-MAS NMR spectrum of **TNP4**, asterisks represent the spinning sideband.

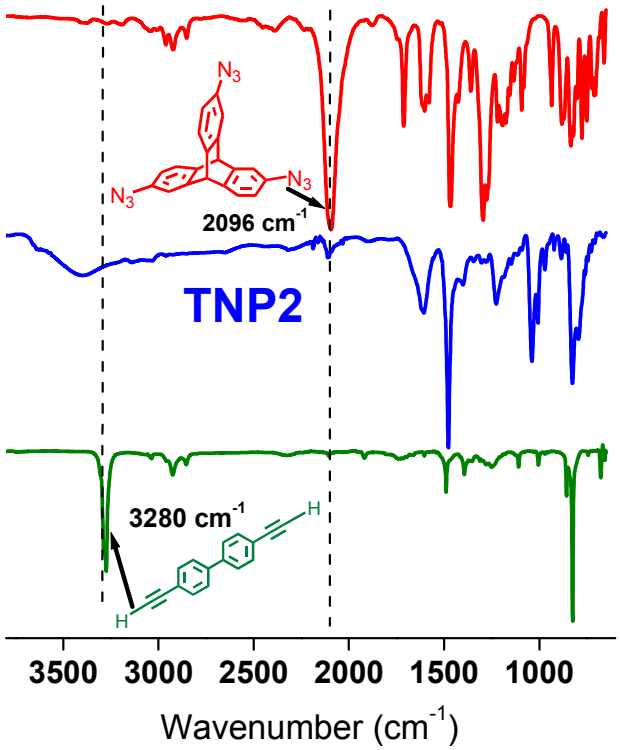

Figure 3. FT-IR spectrum of 2,6,14-triazidotriptycene (top), **TNP2** (middle), and 4,4'-diethynylbiphenyl (bottom).

Porosity Measurements and Gas Storage Studies:

Porous properties of the **TNP**s were investigated by subjecting these polymers to N_2 adsorption-desorption measurements at 77K. The isotherms are characterized by steep increase in slope in low relative pressure range (P/P_0 = 0−0.1) and this implies uptake of large quantities of N_2 gas. Additionally, the isotherms are reversible in nature. These characteristic features of the obtained adsorption-desorption isotherms (Figure 4) suggest that these are Type-I isotherms and the corresponding **TNP** polymers reported herein are microporous materials, as per IUPAC classifications.[63] A gradual increase in N_2 uptake in the relatively high pressure range (P/P_0 = 0.1−0.9) was also observed in these isotherms. In case of all **TNP**s, the adsorption and desorption branches of the hysteresis loop remain almost parallel over an appreciable range of P/P_0, thereby suggesting that these materials (**TNP 1-4**) show type H4 adsorption-desorption hysteresis. According to IUPAC, "the Type H4 loop appears to be associated with narrow slit-like pores, but in this case the Type I isotherm character is indicative of microporosity".[63]

An additional feature observed in the isotherm of **TNP2** and **TNP3** is their steep rise while relative pressure (P/P_0) is greater than 0.9, which is an indication of the presence of larger pores (macropores) and interparticle voids.[24,64] Thus isotherms of **TNP2** and **TNP3** are distinctly different from those of **TNP1** and **TNP4**. It may be recalled that in the FESEM micrographs, **TNP2** and **TNP3** exhibited particle like nature having inter particle porosity, while **TNP1** and **TNP4** exhibit more aggregated plate like morphologies suggesting that these have insignificant inter particle porosity. Thus conclusions drawn from analysis of FESEM micrographs and adsorption-desorption isotherms substantiate each other.

DFT model based analysis results of pore size distributions (PSD) of **TNP**s (calculated from N_2 adsorption data at 77K) are depicted in Figure 4b. In the case of **TNP1** and **TNP4** wherein both comonomers are trifunctional, the pores are smaller than 2 nm. For these polymers, a narrow peak is observed in the ultramicroporous region (pore width < 0.7 nm) at 0.59 nm and 0.57 nm respectively, thereby suggesting presence of ultramicropores in these polymers. The PSD profiles of **TNP2** and **TNP3** also confirm the presence of micropores. Here a major peak is centered at 1.7 nm and 1.6 nm respectively for **TNP2** and **TNP3**. Total pore volume of TNPs (calculated at P/P_0 = 0.99) are in the range of 0.53 to 0.66 cm^3g^{-1}(Table 1). In general, PSD is relatively narrow in case of polymers (**TNP1** and **TNP4**) that utilized both trifunctional monomers relative to polymers (**TNP2** and **TNP3**) where one of the comonomer is bifunctional. These results clearly show that pore size distribution of **TNP**s can be controlled by varying the number of reactive sites in the monomers. The microporous nature of **TNP**s is attributed to presence of rigid three dimensional triptycene motifs in the polymer backbone.

The surface area (SA) of **TNP**s have been obtained using Brunauer−Emmett−Teller (BET) model within the pressure range P/P_0 = 0.01 to 0.1 (Figure S3). The SA_{BET} obtained for **TNP1**, **TNP2**, **TNP3** and **TNP4** are 1090 m^2g^{-1}, 460 m^2g^{-1}, 745 m^2g^{-1} and 1348 m^2g^{-1} respectively. The corresponding Langmuir surface areas are 1475 m^2g^{-1}, 756 m^2g^{-1}, 1006 m^2g^{-1} and 1723 m^2g^{-1} respectively (Table 1 and Figure S4). Polymers **TNP1** and **TNP4** synthesized from triethynyl comonomer exhibit higher surface area relative to the other two polymers (**TNP2** and **TNP3**) where diethynyl comonomer has been utilized for polymerization. This difference in surface area of network polymers (TNP1 and TNP4) resulting from triethynyl monomers relative to polymers (TNP2 and TNP3) derived from disubstituted monomers is attributed to the higher extent of cross-linking as well as difference in the geometry of the comonomers. Irrespective of the nature of ethnyl monomer used in conjugation with 2,6,14-triazidotriptycene, the resulting **TNP**s are significantly porous and their corresponding surface areas (SA_{BET}) are comparable or better than a wide variety of microporous polymers reported in literature such as mPAF (948-1314 m^2g^{-1}),[27] Benzimidazole-Linked Polymers (BILPs, 599-1306 m^2g^{-1}),[25,65,66] imine-linked PPFs (419-1740 m^2g^{-1}),[24] Nitrogen-Doped Microporous Carbons (263-744 m^2g^{-1}),[29] Imine-Linked POFs (466-1521 m^2g^{-1}),[31] nanoporous azo-linked polymers (ALPs, 862-1235 m^2g^{-1}),[32] "click-based'' POPs (1090-1440 m^2g^{-1})[33] and triptycene-based microporous polymers such as benzimidazole network (600 m^2g^{-1}),[56] porous polymer

derived from Tröger's Base (TB-MOP, 694 m^2g^{-1}),[58] and microporous polyimides (STPIs, 4-541 m^2g^{-1}).[54] The surface area and pore properties are summarized in Table 1.

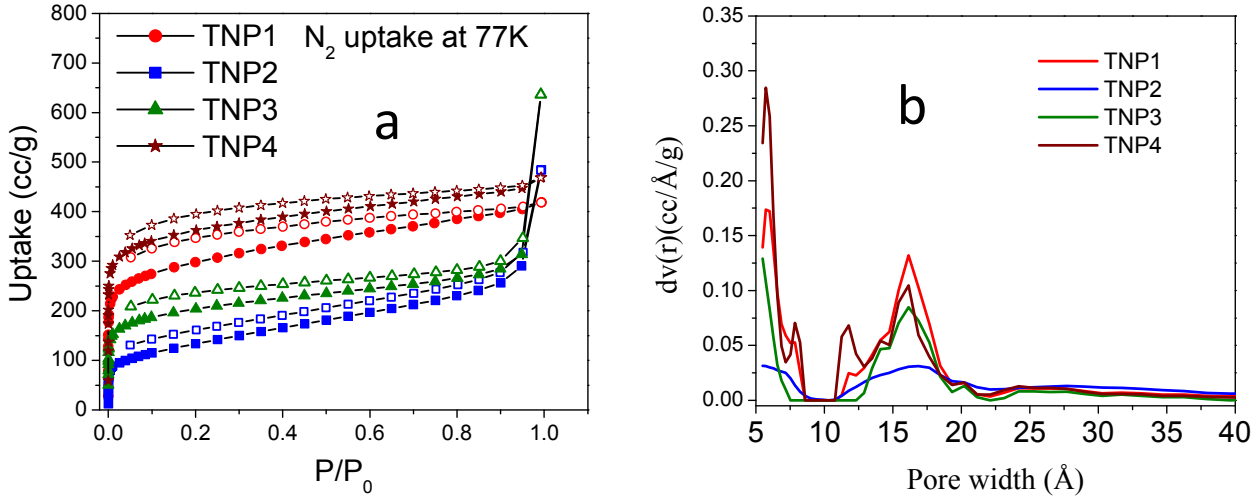

Figure 4. N_2 adsorption isotherm of **TNP1-TNP4** at 77K (a); Pore size distribution of **TNP1-TNP4** (b).

Table 1. Reaction yield and pore properties of **TNP1-TNP4**.

Polymer	SA_{BET} (m^2g^{-1})[a]	SA_{Lang} (m^2g^{-1})[b]	V_{total} ($cm^3\ g^{-1}$)[c]	Yield (%)
TNP1	1090	1475	0.58	96
TNP2	460	756	0.53	88
TNP3	745	1006	0.62	85
TNP4	1348	1723	0.66	98

[a]Surface area calculated based on the BET model from the nitrogen adsorption isotherm (P/P_0 = 0.01-0.1). [b]Surface area calculated based on the Langmuir model from the nitrogen adsorption isotherms (P/P_0 = 0.05-0.35). [c]The total pore volume calculated at P/P_0 = 0.99.

Considering the microporous nature of **TNP**s and the presence of nitrogen-rich 1,2,3-triazole moieties present in the polymer framework, we were interested to investigate the potential of **TNP**s as porous materials for gas storage applications. It has been reported in literature that nitrogen enriched microporous organic polymers perform well as materials for storage of small gas molecules in general and particularly CO_2. Therefore to assess the performance of **TNP**s in selective gas storage materials, adsorption isotherms for CH_4, CO_2, and H_2 were collected under different conditions.

The CO_2 sorption isotherms of **TNP**s were collected at 273 and 298 K and pressures upto 1 bar. The corresponding CO_2 isotherms register a steep rise in the initial low pressure region and are completely reversible in the entire region due to the absence of any significant adsorption-desorption hysteresis [Figure 5a (273K) and Figure S5 (298K)]. The reversibility suggests that interactions between **TNP**s and CO_2 are weak to the extent of regeneration of the polymers without application of heat.[32] As observed in case of N_2 sorption analysis, **TNP**s (**1** and **4**) derived from triethynyl comonomers shows higher uptake of CO_2 relative to **TNP**s (**2** and **3**) derived from diethynyl comonomers. At 273 K and 1.0 bar, **TNP4** demonstrates highest CO_2 uptake of 196 mg/g (4.45 mmol/g), while **TNP2** shows lowest value of CO_2 uptake at 70 mg/g (1.59 mmol/g). Importantly, the magnitude of CO_2 uptake by these **TNP**s is comparable or better than various literature reported COFs. For example, the uptake of **TNP4** (4.45 mmol/g at 273K/1 bar) exceeds this value for −OH functionalized POFs (4.2 mmol/g),[67] imine linked ILP

(1.97 mmol/g),[29] BLP1 (4.27 mmol/g),[65] and tetraphenyladamantane based PAN (3.36-4.0 mmol/g).[37] In general, the CO_2 uptake values (1.59-4.45 mmol/g at 273K/1bar) of **TNP**s are comparable with various microporous organic polymers such as triazine based TBILP (2.66-5.18 mmol/g),[42] microporous covalent triazine polymers (MCTP, 3.65-4.64 mmol/g),[40] and carbazolic porous organic frameworks (Cz-POFs, 1.75-4.77 mmol/g).[38] Furthermore, The CO_2 uptake capacities of these TNPs are comparable to MOFs such as $Zn_2(C_2O_4)(C_2N_4H_3)_2\cdot(H_2O)_{0.5}$ (4.35 mmol g^{-1})[68] and amine-functionalized MOFs such as bio-MOF-11 (6.0 mmol g^{-1}).[69] The observed substantial uptake of CO_2 by these triptycene-based **TNP**s can be considered as a consequence of high internal molecular free volume (IMFV) due to the triptycene units and high nitrogen content due to the triazole motifs. Recently, theoretical studies have shown that 1,2,3-triazole molecules have large CO_2- binding energy (BE) (20.0 kJ mol^{-1}) possibly due to high affinity of triazole rings for CO_2 via strong electrostatic interactions.[51]

To further understand the interaction of CO_2 with **TNP**s, the isosteric heats of adsorption (Q_{st}) for CO_2 in **TNP**s were estimated from the CO_2 adsorption isotherm at 273 and 298 K. The Q_{st} values for CO_2 at zero coverage (at the onset of adsorption) are in the range of 34.8-38.5 KJ/mol. Strong interactions between CO_2 and polar 1,2,3-triazole motifs as well as the narrow distribution in the microporous region may be the reason for high Q_{st} value observed in low pressure region. The Q_{st} values (34.8-38.5 KJ/mol) of **TNP**s are higher than a variety of previously reported porous organic polymers such as nanoporous azo-linked polymers (ALPs: 27.9-29.6 KJ/mol),[32] imine-linked porous polymer frameworks (PPFs: 21.8-29.2 KJ/mol),[24] benzimidazole-linked polymers (BLPs: 26.7-28.0. KJ/mol),[25,65,66] nitrogen-rich networks (PECONFs: 26-34 KJ/mol)[64] nitrogen-rich diaminotriazine-based polymers (APOPs, 26.6-33.3 KJ/mol),[70] and carbazolic porous organic frameworks (Cz-POFs, 24.8-27.8 KJ/mol).[38] However these values are slightly less than microporous covalent triazine polymers (MCTPs, 30.6-40 KJ/mol).[40]

In addition to CO_2, **TNP**s were also investigated as materials for the sorption of other gases such as H_2 and CH_4 (Table 2). CH_4 gas isotherms of **TNP**s were collected at 273K (Figure 5c) and 298 K (Figure S5) up to 1 bar pressure. At 273 K, **TNP4** registers highest methane uptake (23.8 mg/g) while **TNP2** records lowest (10.0 mg/g). Irrespective of extent methane sorption, all the isotherms are completely reversible. We have also calculated the isosteric heat of adsorption (Q_{st}) for methane in **TNP**s and values at zero coverage are found to be in the range of 13.2-20.0 KJ/mol. These magnitudes of Q_{st} are comparable with the various hetero functionalized porous organic polymer.[24,25,27,32]

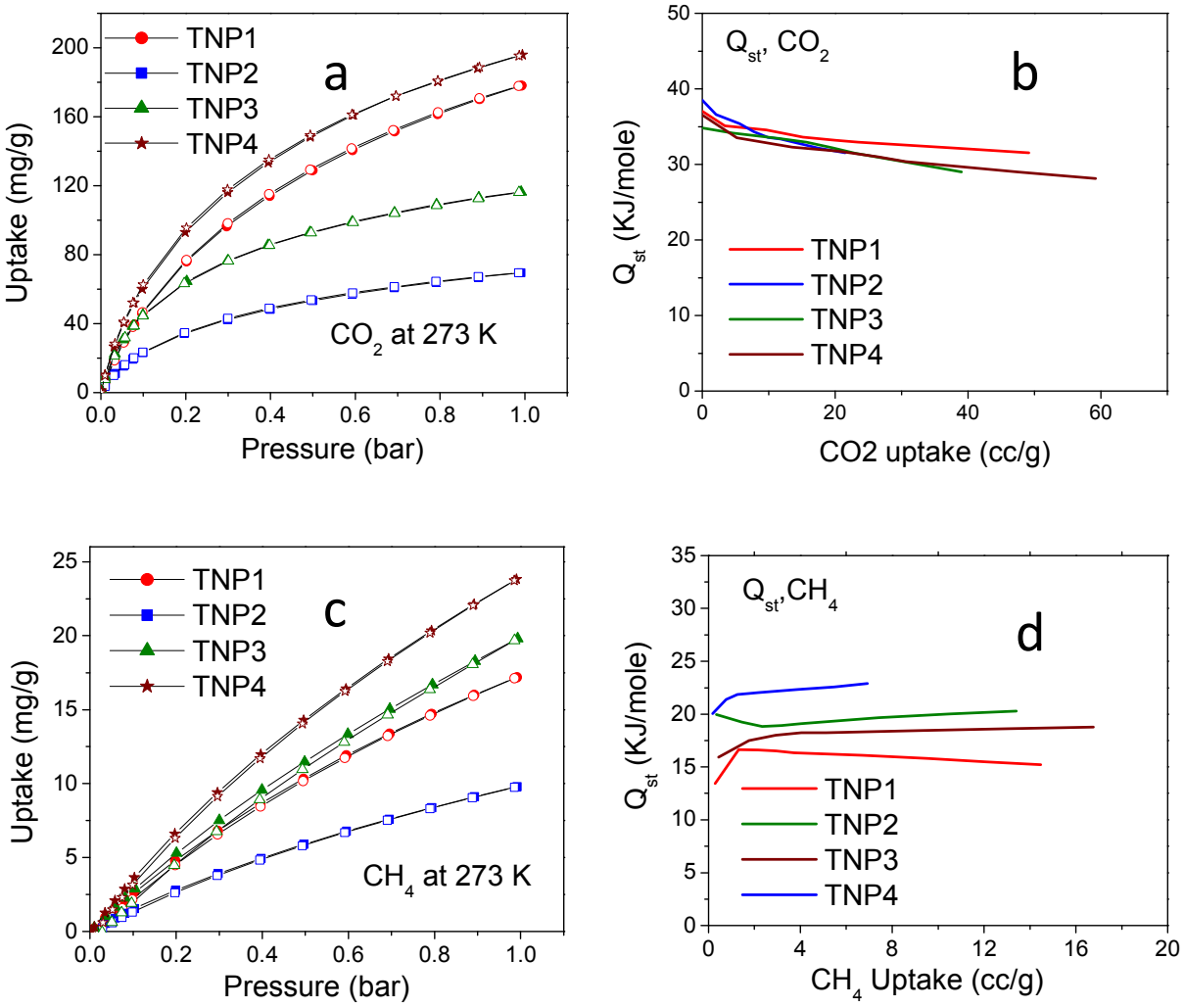

Figure 5. CO_2 uptake isotherm of **TNP1-TNP4** at 273K (a), Isosteric heat of adsorption {Q_{st}} of **TNPs** for CO_2 (b), Methane uptake isotherm of **TNP1-TNP4** at 273K (c) and Q_{st} of **TNPs** for CH_4 (d). Adsorption (filled) and desorption (empty)

Similarly, H_2 adsorption isotherms were collected at 77K for **TNP**s (Figure 6). The uptake capacity of H_2 increases in the order of **TNP2**<**TNP3**<**TNP1**<**TNP4** which is consistent with the increasing order of surface area (SA_{BET}). The H_2 uptakes of **TNP**s are in the range of 0.8-1.8 wt% at 77K and 1bar, which is comparable with various organic porous polymers such as, nanoporous azo-linked polymers (ALPs, 1.39-2.19 wt%),[32] and benzimidazole-linked polymers (BILP1, 1.9%)[65] under identical experimental conditions.

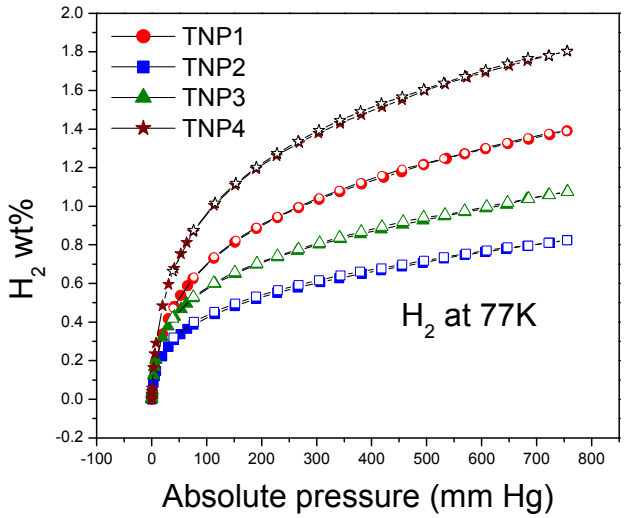

Figure 6. H_2 uptake isotherm of **TNP1-TNP4** at 77K. Adsorption (filled) and desorption (empty)

Table 2. H_2, CO_2, CH_4, and N_2 Uptakes, Isosteric Heats of Adsorption (Q_{st}) for **TNP**s, and selectivity for CO_2/N_2 and CO_2/CH_4.

Polymer	H_2 at 1 bar (77K)	CO_2 at 1 bar (mg/g)			CH_4 at 1 bar (mg/g)			N_2 at 1 bar (mg/g)		Selectivity	
		273K	298K	Q_{st}	273K	298K	Q_{st}	273K	298K	CO_2/N_2 273K(298K)	CO_2/CH_4 273K(298K)
TNP1	14	178	99	37.0	17.3	11.5	13.2	3.4	2.1	36(23)	8(5)
TNP2	8	70	43	38.5	10.0	5.2	20	2.3	1.1	40(23)	8(5)
TNP3	11	116	81	34.8	19.8	10.9	16.2	3.8	2.1	48(31)	9(6)
TNP4	18	196	127	36.5	23.8	14.2	20	7.3	3.2	31(27)	8(6)

Gas Selectivity:

After evaluation of the porosity and gas-uptake capacities of these **TNP**s, we were interested to study their ability to selectively capture CO_2 over CH_4 and N_2. It is well known that in order to reduce environmental pollution due to CO_2 (a green house gas) present in flue gas (N_2/CO_2: 85:15), it is necessary to selectively capture CO_2 over N_2. Also it is well accepted that CO_2 is a contaminant in natural gas (CH_4/CO_2: 95:5) and it is necessary to selectively capture CO_2 over methane in order to improve the quality of natural gas as a fuel and also control corrosion in pipeline due to CO_2.

In order to access the performance of **TNP**s in CO_2/CH_4 and CO_2/N_2 gas selectivities, it is required to record the single component adsorption isotherms of these gases at 273K (Figure 7) and 298K (Figure S6) up to 1 bar pressure. For a given **TNP**, an initial steeper rise in the CO_2 adsorption isotherm in comparison to that in case of corresponding N_2 or CH_4 isotherm was anticipated, considering the higher Q_{st} values of **TNP**s for CO_2 in zero surface coverage (Table 2) due to favorable interactions between CO_2 and N_2 centers present in the 1,2,3-triazole moieties. It must be mentioned here that in flue gas, CO_2 partial pressure is typically 0.15 bar at 273 K.[25] Thus for a given porous material, it is worth considering its relative uptake of gases (CO_2 vs N_2 or CH_4) at 0.15 bar while evaluating its performance in selective

gas adsorption. In case of **TNP**s, at 0.15 bar the adsorption isotherms indicate significantly higher CO_2 uptake relative to N_2 or CH_4. Considering this fact, these **TNP**s can be considered as useful materials for selective CO_2 gas adsorption applications under these conditions.

Subsequently, CO_2/N_2 and CO_2/CH_4 gas selectivity of these **TNP**s was estimated from the initial slope ratios using Henry's law constants for single-component adsorption isotherms (Figure S7 and Figure S8). This method has been routinely used to study gas selectivity properties of a wide variety of organic and inorganic hybrid materials.[25,32]

Therefore, the N_2/CO_2 selectivity of **TNP**s has been calculated from the isotherms recorded at 273K and 298K in the pressure range below 0.15 bar, and the results are summarized in table 2. Overall, the selectivity at 273K (31-48) is higher than the selectivity at 298K (23-31) for all **TNP**s. Amongst these four network polymers, **TNP3** shows highest selectivity for CO_2 over N_2 (48 at 273K). This may be attributed to the presence of additional pyrazine motifs in **TNP3** that are absent in the other three **TNP**s. This polymer (**TNP3**) offers more nitrogen sites for interaction with CO_2 in comparison to the other **TNP**s. The data also suggests a considerable trade-off between gas storage capacity and gas selectivity amonst the four **TNP**s reported herein. For example, **TNP4** having highest surface area (SA_{BET} = 1348 m^2/g), exhibits less selectivity for CO_2 over N_2 (31 at 273K) in comparison to **TNP1** (SA_{BET} = 1090 m^2/g, CO_2/N_2 = 36 at 273K) and **TNP2** (SA_{BET} = 460 m^2/g, CO_2/N_2 = 40 at 273K). In general, the **TNP** with a relatively higher surface area exhibited relatively lower CO_2/N_2 selectivity. **TNP3** is an exception since it has higher nitrogen content in comparison to the other **TNP**s. Thus our results corroborate with the general perception that higher porosity level accompanies with a compromise in CO_2/N_2 selectivity.[25,32] Nevertheless, the CO_2/N_2 selectivity of these 1,2,3-triazole linked network polymers (**TNP**s) are better than a wide range of microporous materials reported in literature.[32,35-38,41,70]

Additionally, the CO_2/CH_4 selectivity of **TNP**s was also investigated to ascertain their applicability in the purification on natural gas (CH_4/CO_2: 95:5) by capture of CO_2. Methane adsorption isotherms were collected at 273K and 298K and selectivity was determined using the initial slope calculation, and the results obtained are depicted in table 2. CO_2/CH_4 selectivities at 273K and 1bar are in the range of 8-9. At a higher temperature (298K), the CO_2/CH_4 selectivity was found to decrease to 5-6. In general, the **TNP**s exhibit significantly lower CO_2/CH_4 selectivity relative to CO_2/N_2 selectivity. It is reported that due to higher polarizability of methane relative to N_2, adsorption potential of methane is much higher than that of N_2 and this may be the explanation for the observed lower CO_2/CH_4 selectivities in comparison to CO_2/N_2 selectivities.[32]

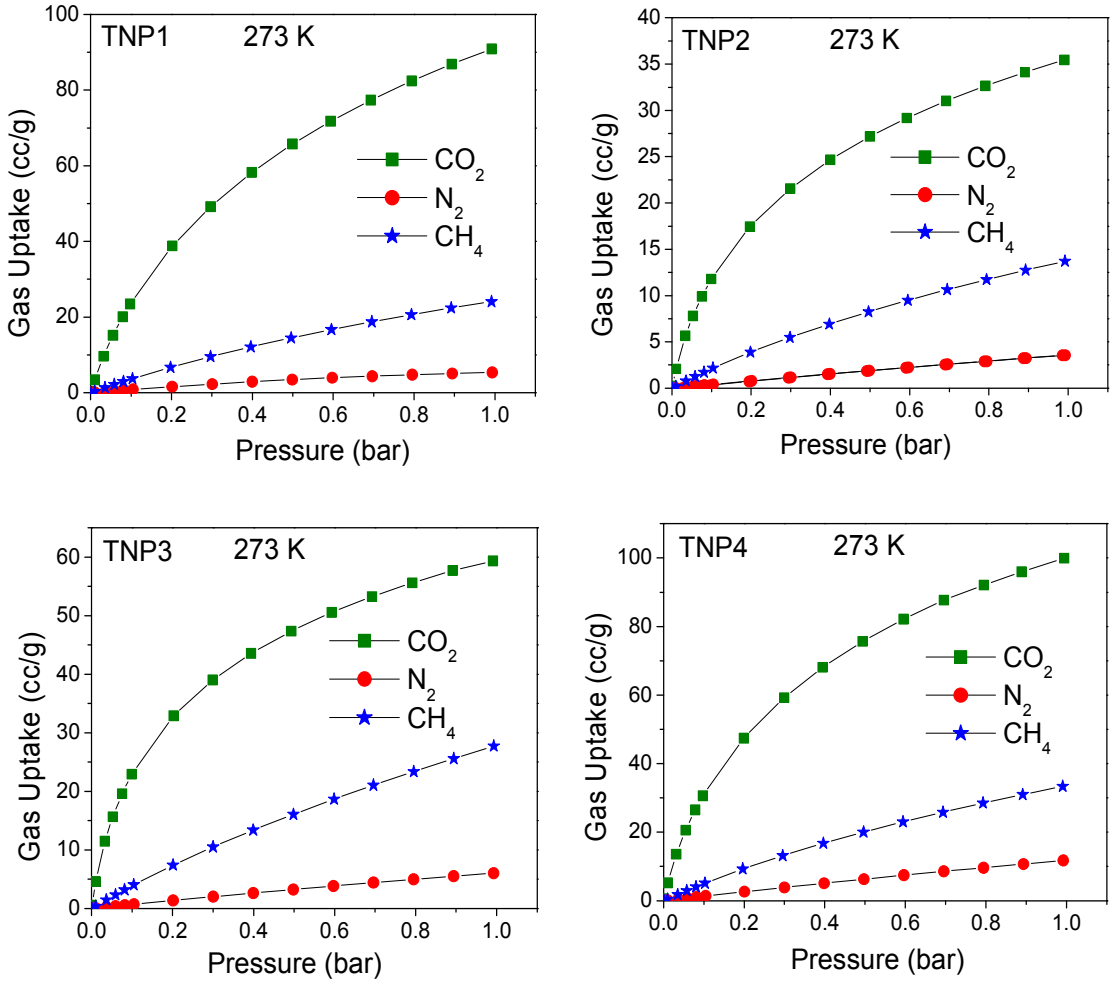

Figure 7. Gas uptake capacities for **TNP1-TNP4** at 273 K. CO_2 (green square), CH_4 (blue star), and N_2 (red circle).

Conclusion:

In conclusion, facile synthesis and characterization of a series of triptycene based and 1,2,3-triazole laced alternating copolymers has been described. The resulting 1,2,3-Triazole linked Network Polymers (**TNP**s) are microporous materials exhibiting BET surface area up to 1348 m^2g^{-1}. We have also shown that incorporation of nitrogen-rich pyrazine moieties results in enhancement of CO_2/N_2 gas selectivity relative to **TNP**s that do not possess this hetero-aromatic structural motif in the polymer backbone. In general, we have shown that integration of triptycene and 1,2,3-triazole motifs in the backbone of organic network polymer results in the yield of materials that demonstrate excellent performance in storage of small gases at low pressure. Considering the microporosity, large gas uptake and high selectivities of CO_2 over N_2 and CH_4, **TNP**s are potential candidates for practical applications such as CO_2 capture as well as purification of flue and natural gas. Currently, we are extending our research in the direction of facile synthesis of novel microporous organic polymers with applications in clean energy sector by utilizing new multifunctional monomers for tailoring the gas sorption properties.

Acknowledgements

N.D. thanks the CSIR, Govt. of India, New Delhi [CSIR No. 02(0126)/13/EMR-II] for financial support. S.M. thanks UGC, New Delhi for a Research Fellowship. Authors acknowledge Indian Institute of Technology Patna for providing infrastructure required for this research. The authors also acknowledge Central NMR Facility, CSIR-NCL for acquiring ^{13}C CP-MAS data**.**

Appendix A. Supplementary data

Supplementary data related to this article can be found at http://.....

References

1. K. Sumida, D. L. Rogow, J. A. Mason, T. M. McDonald, E. D. Bloch, Z. R. Herm, T. Bae and J. R. Long, *Chem. Rev.* 2012, **112**, 724-781.
2. B. Chen, S. Xiang and G. Qian, *Acc. Chem. Res.* 2010, **43**, 1115-1124.
3. J.-R. Li, Y.-G. Ma, M. C. McCarthy, J. Sculley, J.-M. Yu, H.-K. Jeong, P. B. Balbuena and H.-C. Zhou, *Coord*. *Chem. Rev.* 2011, **255**, 1791-1823.
4. W. Zhou, *Chem. Rec.* 2010, **10**, 200-204.
5. Z. Zhang, Z.-Z. Yao, S. Xiang and B. Chen, *Energy Environ. Sci.* 2014, **7**, 2868-2899.
6. W. Shen and W. Fan, *J. Mater. Chem. A* 2013, **1**, 999-1013.
7. T. A. Makal, J.-R. Li, W. Lu and H.-C. Zhou, *Chem. Soc. Rev.* 2012, **41**, 7761-7779.
8. Z. Xiang and D. Cao, *J. Mater. Chem. A* 2013, **1**, 2691-2718.
9. S.-Y. Ding and W. Wang, *Chem. Soc. Rev.* 2013, **42**, 548-568.
10. K. Sakaushi and M. Antonietti, *Acc. Chem. Res.* 2015, **48**, 1591-1600.
11. M. L. Foo, R. Matsuda and S. Kitagawa, *Chem. Mater.* 2014, **26**, 310-322.
12. (a) Y. Xu, S. Jin, H. Xu, A. Nagai and D. Jiang, *Chem. Soc. Rev.* 2013, **42**, 8012-8031. (b) X. Feng, X. Dinga and D. Jiang, *Chem. Soc. Rev.* 2012, **41**, 6010-6022.
13. Z. Chang, D.-S. Zhang, Q. Chen and X.-H. Bu, *Phys. Chem. Chem. Phys.* 2013, **15**, 5430-5442.
14. S.-Y. Lee and S.-J. Park, *J. Anal. Appl. Pyrolysis* 2014, **106**, 147-151.
15. R. Swaidan, M. Al-Saeedi, B. Ghanem, E. Litwiller and I. Pinnau, *Macromolecules* 2014, **47**, 5104-5114.
16. B. S. Ghanem, R. Swaidan, E. Litwiller and I. Pinnau, *Adv. Mater.* 2014, **26**, 3688-3692.
17. A. Corma, *Chem. Rev.* 1997, **97**, 2373-2419.
18. R. Ryoo, S. H. Joo, M. Kruk and M. Jaroniec, *Adv. Mater.* 2001, **13**, 677-681.
19. F. Hoffmann, M. Cornelius, J. Morell and M. Froeba, *Angew. Chem. Int. Ed.* 2006, **45**, 3216-3251.
20. A. R. Studart, U. T. Gonzenbach, E. Tervoort and L. J. Gauckler, *J. Am. Ceram. Soc.* 2006, **89**, 1771-1789.
21. O. Okay, *Prog. Polym. Sci.* 2000, **25**, 711-779.
22. M. E. Davis and R. F. Lobo, *Chem. Mater.* 1992, **4**, 756-68.
23. J. Caro, M. Noack, P. Kolsch and R. Schafer, *Microporous Mesoporous Mater.* 2000, **38**, 3-24.
24. Y. Zhu, H. Long and W. Zhang, *Chem. Mater.* 2013, **25**, 1630-1635.
25. M. G. Rabbani and H. M. El-Kaderi, *Chem. Mater.* 2012, **24**, 1511-1517.
26. W. Lu, D. Yuan, J. Sculley, D. Zhao, R. Krishna and H.-C. Zhou, *J. Am. Chem. Soc.* 2011, **133**, 18126-18129.
27. M. Errahali, G. Gatti, L. Tei, G. Paul, G. A. Rolla, L. Canti, A. Fraccarollo, M. Cossi, A. Comotti, P. Sozzani and L. Marchese, *J. Phys. Chem. C* 2014, **118**, 28699-28710.
28. M. Saleh, S. B. Baek, H. M. Lee and K. S. Kim. *J. Phys. Chem. C* 2015, **119**, 5395-5402.

29. J. Wang, I. Senkovska, M. Oschatz, M. R. Lohe, L. Borchardt, A. Heerwig, Q. Liu and S. Kaskel. *ACS Appl. Mater. Interfaces* 2013, **5**, 3160-3167.
30. V. M. Suresh, S. Bonakala, H. S. Atreya, S. Balasubramanian and T. K. Maji, *ACS Appl. Mater. Interfaces* 2014, **6**, 4630-4637
31. P. Pandey, A. P. Katsoulidis, I. Eryazici, Y. Wu, M. G. Kanatzidis and S. T. Nguyen, *Chem. Mater.* 2010, **22**, 4974-4979.
32. P. Arab, M. G. Rabbani, A. K. Sekizkardes, T. İslamoğlu and H. M. El-Kaderi, *Chem. Mater.* 2014, **26**, 1385-1392.
33. P. Pandey, O. K. Farha, A. M. Spokoyny, C. A. Mirkin, M. G. Kanatzidis, J. T. Hupp and S. T. J. Nguyen, *Mater. Chem.* 2011, **21**, 1700-1703
34. Y.-S. Bae and R. Q. Snurr, *Angew. Chem. Int. Ed.* 2011, **50**, 11586-11596.
35. Z. Wang, D. Wang, F. Zhang and J. Jin, *ACS Macro Lett.* 2014, **3**, 597-601.
36. H. J. Jo, C. Y. Soo, G. Dong, Y. S. Do, H. H. Wang, M. J. Lee, J. R. Quay, M. K. Murphy and Y. M. Lee, *Macromolecules* 2015, **48**, 2194-2202.
37. G. Li, B. Zhang, J. Yan and Z. Wang, *Macromolecules* 2014, **47**, 6664-6670.
38. X. Zhang, J. Lu and J. Zhang, *Chem. Mater.* 2014, **26**, 4023-4029.
39. Y.-Q. Shi, J. Zhu, X.-Q. Liu, J.-C. Geng and L.-B. Sun, *ACS Appl. Mater. Interfaces* 2014, **6**, 20340-20349.
40. P. Puthiaraj, S.-M. Cho, Y.-R. Lee and W.-S. Ahn, *J. Mater. Chem. A* 2015, **3**, 6792-6797.
41. Y. Zhuang, J. G. Seong, Y. S. Do, H. J. Jo, Z. Cui, J. Lee, Y. M. Lee and M. D. Guiver, *Macromolecules* 2014, **47**, 3254-3262.
42. A. K. Sekizkardes, S. Altarawneh, Z. Kahveci, T. İslamoğlu and H. M. El-Kaderi, *Macromolecules* 2014, **47**, 8328-8334.
43. M. Salehab and K. S. Kim, *RSC Adv*. 2015, **5**, 41745-41750.
44. B. Ashourirad, A. K. Sekizkardes, S. Altarawneh and H. M. El-Kaderi, *Chem. Mater.* 2015, **27**, 1349-1358.
45. M. Yu, X. Wang, X. Yang, Y. Zhao and J.-X. Jiang, *Polym. Chem.* 2015, **6**, 3217-3223
46. R. Dawson, E. Stöckel, J. R. Holst, D. J. Adams and A. I. Cooper, *Energy Environ. Sci.* 2011, **4**, 4239-4245.
47. S. Chu, *Science* 2009, **325**, 1599.
48. R. S. Haszeldine, *Science* 2009, **325**, 1647-1652.
49. X. Lu, D. Jin, S. Wei, Z. Wang, C. An, W. Guo, *J. Mater. Chem. A* 2015, **3**, 12118-12132.
50. Y.-S. Bae and R. Q. Snurr, *Angew. Chem. Int. Ed.* 2011, **50**, 11586-11596.
51. H. M. Lee, I. S. Youn, M. Saleh, J. W. Lee and K. S. Kim, *Phys. Chem. Chem. Phys.* 2015, **17**, 10925-10933.
52. C. Zhang, Y. Liu, B. Li, B. Tan, C.-F. Chen, H.-B. Xu and X.-L. Yang, *ACS Macro Lett.* 2012, **1**, 190-193.
53. (a) M. Carta, M. Croad, R. Malpass-Evans, J. C. Jansen, P. Bernardo, G. Clarizia, K. Friess, M. Lanč and N. B. McKeown, *Adv. Mater.*, 2014, **26**, 3526-3531. (b) B. S. Ghanem, M. Hashem, K. D. M. Harris, K. J. Msayib, M. Xu, P. M. Budd, N. Chaukura, D. Book, S. Tedds, A. Walton and N. B. McKeown, *Macromolecules*, 2010, **43**, 5287–5294.
54. C. Zhang, T.-L. Zhai, J.-J. Wang, Z. Wang, J.-M. Liu, B. Tan, X.-L. Yang and H.-B. Xu, *Polymer* 2014, **55**, 3642-3647.
55. T. M. Swager, *Acc. Chem. Res.* 2008, **41**, 1181−1189.
56. Y. He, X. Zhu, Y. Li, C. Peng, J. Hu and H. Liu, *Microporous Mesoporous Mater.* 2015, **214**, 181-187.
57. Q. Wen, T.-Y. Zhou, Q.-L. Zhao, J. Fu, Z. Ma and X. Zhao, *Macromol. Rapid Commun.* 2015, **36**, 413−418.
58. X. Zhu, C.-L. Do-Thanh, C. R. Murdock, K. M. Nelson, C. Tian, S. Brown, S. M. Mahurin, D. M. Jenkins, J. Hu, B. Zhao, H. Liu and S. Dai, *ACS Macro Lett.* 2013, **2**, 660-663.

59. Chakraborty, S.; Mondal, S.; Kumari, R.; Bhowmick, S.; Das, P.; Das, N. *Beilstein J. Org. Chem.* **2014**, *10*, 1290-1298.
60. (a) M. I. Mangione, R. A. Spanevello, A. Rumbero, D. Heredia, G. Marzari, L. Fernandez, L. Otero and F. Fungo, *Macromolecules*, 2013, **46**, 4754−4763. (b) S. Chakraborty, S. Mondal, N. Das, *Inorg. Chim. Acta*, 2014, **413**, 214-220. (c) S. Bhowmick, S. Chakraborty, A. Das, P. R. Rajamohanan, and N. Das, *Inorg. Chem.*, 2015, **54**, 2543-2550. (d) S. Yuan, B. Dorney, D. White, S. Kirklin, P. Zapol, L. Yu and D.-J. Liu, *Chem. Commun.*, 2010, **46**, 4547-4549.
61. A. Qin, J. W. Y. Lam and B. Z. Tang, *Macromolecules* 2010, **43**, 8693-8702.
62. Y. Chen and Z. Guan, *J. Am. Chem. Soc*., 2010, **132**, 4577-4579.
63. K. S. W. Sing, *Pure Appl. Chem.* 1982, **54**, 2201-2218.
64. P. Mohanty, L. D. Kull and K. Landskron, *Nat. Commun.* 2011, DOI: 10.1038/ncomms1405.
65. M. G. Rabbani and H. M. El-Kaderi, *Chem. Mater.* 2011, **23**, 1650-1653.
66. M. G. Rabbani, T. E. Reich, R. M. Kassab, K. T. Jackson and H. M. El-Kaderi, *Chem. Commun.* 2012, **48**, 1141-1143.
67. A. P. Katsoulidis and M. G. Kanatzidis, *Chem. Mater.* 2011, **23**, 1818-1824.
68. R. Vaidhyanathan, S. S. Iremonger, K. W. Dawson, and G. K. H. Shimizu, *Chem. Commun.* 2009, **45**, 5230–5232.
69. J. An, S. J. Geib, and N. L. Rosi, *J. Am. Chem. Soc.* 2010**, 132,** 38–39.
70. W.-C. Song, X.-K. Xu, Q. Chen, Z.-Z. Zhuang and X.-H. Bu, *Polym. Chem.* 2013, **4**, 4690-4696.